Rojas, E., & Rudy, E. (1976) *J. Physiol. (London) 262*, 502–531.
Tanford, C. F., & Reynolds, J. A. (1976) *Biochim. Biophys. Acta 457*, 133–170.
Trams, E. G., & Hoiberg, C. P. (1970) *Proc. Soc. Exp. Biol. Med. 135*, 193–196.
Ulbricht, W., & Wagner, H.-H. (1975) *Philos. Trans. R. Soc. London, Ser. B 270*, 353–364.

Electrostatic Effects in Hemoglobin: Hydrogen Ion Equilibria in Human Deoxy- and Oxyhemoglobin A†

James B. Matthew,‡ George I. H. Hanania,§ and Frank R. N. Gurd*

ABSTRACT: The modified Tanford–Kirkwood theory of Shire et al. [Shire, S. J., Hanania, G. I. H., & Gurd, F. R. N. (1974) *Biochemistry 13*, 2967] for electrostatic interactions was applied to the hydrogen ion equilibria of human deoxyhemoglobin and oxyhemoglobin. Atomic coordinates for oxyhemoglobin were generated by the application of the appropriate rigid rotation function to α and β chains of the deoxyhemoglobin structure [Fermi, G. (1975) *J. Mol. Biol. 97*, 237]. The model employs two sets of parameters derived from the crystalline protein structures, the atomic coordinates of charged amino acid residues and static solvent accessibility factors to reflect their individual degrees of exposure to solvent. Theoretical titration curves based on a consistent set of pK_{int} values compared closely with experimental potentiometric curves. Theoretical pK values at half-titration for individual protein sites corresponded to available observed values for both quaternary states. The results bring out the cumulative effects of numerous electrostatic interactions in the tetrameric structures and the major effects of the quaternary transition that result from changes in static solvent accessibility of certain ionizable groups.

The classical treatment of hydrogen ion titration curves of proteins regards the molecule as an impenetrable sphere on which amino acid residues are grouped into classes of intrinsically identical sites with their charges uniformly distributed over the surface (Linderstrøm-Lang, 1924). The elegant simplicity of this frequently used model is offset by its inability to yield electrostatic information about individual groups, their specific roles, and their interactions.

In the more realistic discrete-charge electrostatic theory (Tanford & Kirkwood, 1957; Tanford, 1957), the amino acid groups are point charges positioned at fixed sites on the surface of the protein or are buried a short distance within the interior of the molecule which is assumed to be a continuous medium of low dielectric constant. The theory was successfully tested on a variety of model compounds. An early application to hemoglobin was the calculation of electrostatic contributions to the free energy and enthalpy of acid dissociation of the iron-bound H_2O in human ferrihemoglobins A, S, and C; however, this calculation was limited to the mutual effect of two groups only, the iron atom and the amino acid concerned in the substitution (Beetlestone & Irvine, 1964). A full treatment of the hydrogen ion titration curve for tetrameric human hemoglobin was carried out by Orttung (1968, 1969, 1970), although the numerical work was prohibitive. Whereas previous treatments had required burial of the charges up to 1 Å into the low dielectric medium beneath the surface of the molecule, Orttung found that in order to obtain proper fit of the data it was necessary to place all charges at the surface of the hemoglobin molecule. A much more efficient iterative algorithm was developed by Tanford & Roxby (1972) who applied it in analyzing the hydrogen ion titration curve of lysozyme, all charges being assumed in this case to be buried at a uniform depth of 0.4 Å.

In an attempt to overcome the uncertainty over the burial parameter and to allow for the irregular surface of a real protein, Shire et al. (1974a,b, 1975) introduced a modification into the Tanford model whereby, for each individual group, the magnitude of electrostatic intramolecular interaction was reduced in direct proportion to the extent of the group's exposure to the solvent. The degree of exposure of each group is measured by its solvent accessibility parameter (Lee & Richards, 1971). On this new basis, it was shown that the discrete-charge model can be fruitfully employed to study several aspects of electrostatic effects in myoglobin. The theory correctly predicts the individual pK values, determined independently from proton NMR measurements, for histidine ionizations in 12 distinguishable myoglobin species including several histidine residues that are not present in the reference sperm whale myoglobin structure (Botelho et al., 1978). By use of appropriate crystallographic data, the theory has also been shown to account for the hydrogen ion titration behavior of human hemoglobin α chain as well as cytochrome c (Matthew et al., 1978b).

In the present work, the modified Tanford–Kirkwood theory is applied in a detailed study of electrostatic effects in hemoglobin. The generality of this approach is illustrated by the fact that all computations are based on the same consistent set of intrinsic pK values already used (Matthew et al., 1978b; Botelho et al., 1978), with the appropriate solvent accessibility parameter obtained from the known atomic coordinates (Matthew et al., 1978a). The atomic coordinates are derived from a 2.5-Å resolution electron density map of human deoxyhemoglobin (Fermi, 1975). Since corresponding crys-

† From the Department of Chemistry, Indiana University, Bloomington, Indiana 47405. *Received November 9, 1978; revised manuscript received February 16, 1979.* This is the 104th paper in a series dealing with coordination complexes and catalytic properties of proteins and related substances. For the preceding paper see Wittebort et al. (1979). This work was supported by U.S. Public Health Service Research Grant HL-05556. J.B.M. was supported by U.S. Public Health Service Grant T01 GM-1046.

‡ Present address: Department of Molecular Biophysics and Biochemistry, Yale University, New Haven, CT.
§ Present address: Department of Chemistry, American University of Beirut, Beirut, Lebanon.

0006-2960/79/0418-1919$01.00/0

tallographic data are not available for human oxyhemoglobin, atomic coordinates for the latter were derived by rigid rotation and translation of the deoxyhemoglobin α and β chains into the oxyhemoglobin quaternary structure (Muirhead et al., 1967; Cox, 1967). An efficient FORTRAN computer program allows consideration of any globular structure, including the hemoglobin tetramer which has 182 titrable sites. The overall titration curves for deoxy- and for oxyhemoglobin are accurately reproduced when allowance is made for chloride binding (de Bruin et al., 1974; Rollema et al., 1975). The treatment also enables one to compare computed pK values for individual histidine groups with experimentally determined quantities and to interpret the electrostatic role of charge-bearing groups under varying conditions of pH, ionic strength, and concentration of ligand effectors.

Theoretical Section

Electrostatic Free Energy. The Debye–Hückel theory is used in calculating the electrostatic free energy of interaction for a set of discrete point charges on a sphere of radius b and ion exclusion radius a, where $a - b$ is the distance of closest approach of counterion to the protein molecule. The charges are conventionally placed on the surface of the equivalent sphere which is assumed to form a continuous medium with a low internal dielectric constant, D_i, surrounded by solvent water with an external dielectric constant, D.

The first stage of the calculation, for a given set of the parameters a, b, D_i, D, temperature, and ionic strength involves computation of a table of the magnitude of free energy of interaction, W_{ij}, for a pair of unit point charges z_i and z_j placed on the sphere at a separation r_{ij}. Following the formalism of Tanford & Kirkwood (1957), W_{ij} is given by

$$W_{ij} = e^2 z_i z_j [[(A_{ij} - B_{ij})/b] - (C_{ij}/a)] \qquad (1)$$

where e is the electronic charge and A_{ij} and B_{ij}, defined in eq 2, represent the contribution to electrostatic free energy at zero

$$A_{ij} = b/D_i r_{ij}$$

$$B_{ij} = \frac{1 - 2\delta + 2\delta^2}{D_i\left[1 - 2\left(\frac{r_i r_j}{b^2}\right)\cos\theta_{ij} + \left(\frac{r_i r_j}{b^2}\right)^2\right]^{1/2}} + \frac{\delta - 3\delta^2}{\left(D_i \frac{r_i r_j}{b^2}\right)} \ln \times$$

$$\left\{\frac{\left[1 - 2\left(\frac{r_i r_j}{b^2}\right)\cos\theta_{ij} + \left(\frac{r_i r_j}{b^2}\right)^2\right]^{1/2} + \left(\frac{r_i r_j}{b^2}\right) - \cos\theta_{ij}}{1 - \cos\theta_{ij}}\right\} +$$

$$\frac{\delta^2}{D_i} \sum_{n=0}^{\infty} \frac{\left(\frac{r_i r_j}{b^2}\right)^n}{(n+1)^2} P_n(\cos\theta_{ij})$$

$$C_{ij} = \frac{1}{D}\left\{\frac{\kappa a}{1 + \kappa a} + \sum_{n+1}^{\infty} \frac{2n+1}{2n-1}\left[\frac{D}{(n+1)D + nD_i}\right]^2 \times \right.$$

$$\left.\left[\frac{(\kappa a)^2\left(\frac{r_i r_j}{a^2}\right)^n P_n(\cos\theta_{ij})}{\frac{K_{n+1}\kappa a}{K_{n-1}\kappa a} + \frac{n(D - D_i)}{(n+1)D + nD_i}\left(\frac{b}{a}\right)^{2n+1}\frac{(\kappa a)^2}{4n^2 - 1}}\right]\right\} \qquad (2)$$

ionic strength and are functions of the model parameters b, D_i, and D (and hence the ratio $\delta = D_i/D$), as well as the distance between the two point charges, r_{ij}, and the angle subtended by them at the center of the sphere. The term C_{ij} represents the additional contribution at finite ionic strength; it is a function of another two parameters, the ion exclusion radius a and the ionic strength term κ. P_n is a Legendre polynomial of order n.

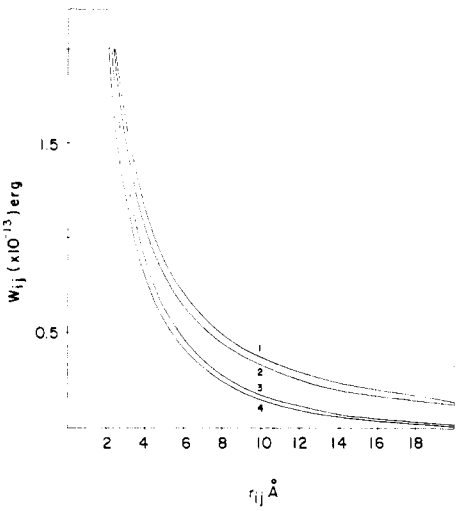

FIGURE 1: Plots of computed electrostatic free energy, W_{ij}, in units of 10^{-13} erg, for two charges i and j placed on a sphere at a separation distance r_{ij}. T = 25 °C; dielectric constant D = 78.5 and D_i = 4.0. Four curves are shown: (1) I = 0.0 M, b = 27.0 Å; (2) I = 0.0 M, b = 18.0 Å; (3) I = 0.10 M, b = 27.0 Å, a = 29.0 Å; and (4) I = 0.10 M, b = 18.0 Å, a = 20.0 Å. b is the radius of the sphere and a is the distance of closest approach of counterions. The 27.0-Å sphere corresponds to the hemoglobin tetramer equivalent sphere, while an 18.0-Å radius would correspond to a monomer equivalent sphere.

Figure 1 illustrates the direct application of this calculation to two cases which are spheres of radii 27 and 18 Å, corresponding to hemoglobin tetramer and monomer, respectively (Orttung, 1970; Fermi, 1975). The plot shows the variation of W_{ij} with separation distance r_{ij}, at D_i = 4.0. As Figure 1 shows, interaction energy is only slightly reduced on decreasing the size of the sphere (curves 1 and 2) but is substantially lowered upon raising the ionic strength from zero to 0.1 (curves 3 and 4). It is a very sensitive function of r_{ij}. Detailed computations for the whole molecule show that the overall effect is the sum of a large number of varying contributions, mostly small but not negligible, and that these summations of small contributions may equal or exceed the individually larger effects of closely positioned groups.

Incorporation of Solvent Accessibility Parameter. The assumption of a fixed dielectric constant gives an oversimplified description of the real interactions at the irregular protein–solvent interface. In our modification of the Tanford model (Shire et al., 1974a), a solvent accessibility parameter (SA), specific for each group and readily computable from given atomic coordinates, is incorporated into the calculation of W_{ij}. The premise here is that individual groups sense a different effective dielectric constant (Hill, 1956), a variability that must be taken into account.

The effective internal dielectric constant to calculate W_{ij} may be defined by a direct relation such as $D(SA_j)$, where D = 78.5 for water at 25 °C, and SA_j is a fraction less than 1. A practical limit for static accessibility of 0.98 will then correspond to substantially complete solvation of the site, and 0.02 will indicate, conversely, nearly complete restriction from the dielectric interface. D_i values could then be used in computing the functions A_{ij}, B_{ij}, and C_{ij} for each group separately. The procedure is inefficient. Moreover, if D_i is not always much less than D, the expansion of B_{ij} in terms of D_i/D requires extension beyond the second power, making the

Table I: Comparison of Some W_{ij} Values (10^{-16} erg) at $I = 0.10$ for Two Methods of Individual Site Static Accessibility Incorporation

	method 1[a]			method 2[b]		
r_{ij} (Å)	SA = 0.05	SA = 0.25	SA = 0.50	D_i = 4.0	D_i = 20.0	D_i = 40.0
4.0	839.5	662.8	441.9	883.7	762.9	599.0
10.0	169.1	133.5	89.0	178.5	173.2	159.4
15.0	62.3	49.2	32.8	65.5	71.6	75.4
54.0	0.17	0.14	0.09	0.18	1.3	3.6

[a] Method 1 shows the W_{ij} values for four values of r_{ij} by using the linear reduction of W_{ij} where $D_i = 4.0$ by the factor $1 - SA$, as adopted. [b] Method 2 shows the corresponding calculated W_{ij} values when the internal dielectric constant used in eq 2 is related to the external dielectric, $D_i = D(SA)$. For all cases the external dielectric constant, D, was 78.5. Sphere radius was 27 Å.

computation even less practical. We have therefore adopted (Shire et al., 1974a) a much simpler linear approximation for the resulting effective electrostatic interaction defined by the relation

$$W'_{ij} = W_{ij}(1 - SA_j) \quad (3)$$

The calculation of W_{ij} values for unit charges was described above; a systematic procedure for calculating SA_j has also been described (Matthew et al., 1978a). Equation 3 implies a reduction of electrostatic free energy for each group in direct proportion to its accessibility to the solvent. This is physically approximately equivalent to assigning an effective dielectric constant in each case. Comparison of the two methods (Table I) shows that the calculated electrostatic free energies are, on the whole, equivalent (Matthew, 1978).

Calculation of pK_i Values. The next stage involves the calculation of the effective pK_i value for a particular site i, with charge $Z_i = +1$ or -1, at fixed pH and ionic strength, as determined by its overall interactions with the other sites j where Z_j assumes fractional values between ± 1 and 0. Thus, reintroducing the fractional charge,[1] Z_j

$$pK_i = (pK_{int})_i - 1/(2.303kT)\sum_{j \neq i} Wm_{ij} z_i Z_j \quad (4)$$

where the electrostatic free energy of interaction with a given group i (eq 3) is summed over all groups j and $(pK_{int})_i$ is the intrinsic ionization constant of the group as obtained from measurements on model compounds that have no intramolecular electrostatic interactions. An iterative procedure (Tanford & Roxby, 1972; Shire et al., 1974a,b; Matthew, 1978; Matthew et al., 1978b) enables the computation of the effective charges Z_i and the pK_i values for all charged groups on the protein under their mutual electrostatic influence. The pK_i of almost every group is found to vary with pH, particularly so at lower ionic strength where interactions are stronger. For this reason, it is convenient to define the parameter $pK_{1/2}$ for a group, this being the pH at which a particular group is half-titrated at a given temperature and ionic strength. It is also noteworthy that the variations in pK_i can be quite substantial, depending on the proximity of charge-bearing groups and the extent of their burial within the protein.

[1] Z_j replaces the unit charge convention (Z_j) employed in eq 1 for the calculation of W_{ij}, implicit in the calculation of W_{ij}' in eq 3 for fully occupied sites. While the total electrostatic work done in placing all the charged sites on the molecule, W, is dependent on the fractional occupancy, Z_i and Z_j, and SA values of all the i and j sites, the derivative dW/dZ_i in the expression for pK_i (Tanford, 1961) is independent of the Z_i value. Consequently, the changes in the pK_i are determined by the signs of z_i and z_j and the fractional occupancy, Z_j.

Theoretical Titration Curves. The variation of Z_i with pH yields the calculated titration curve of a group i in the protein. The sum of all the charges gives the net protein charge as a function of pH, the titration curve of the protein.

Application to Hemoglobin

Site Coordinates. Orthogonal atomic coordinates for human adult deoxyhemoglobin were obtained from the Brookhaven Protein Data Bank listing of the crystal structure determination at 2.5-Å resolution (Fermi, 1975). The data describe the $\alpha\beta$ dimer. Atomic coordinates for the tetramer were generated by reflection across the twofold rotation axis into the spheroidal structure of radius about 27 Å. Corresponding atomic coordinates for human oxyhemoglobin are not available and had to be derived. Rigid rotation of the deoxyheoglobin α and β chains into the oxyhemoglobin quaternary structure required the use of the inverse of the rotation matrix specified by the Eulerian angles and inverse of the translation components for the oxy- to deoxyhemoglobin transformation (Muirhead et al., 1967; Cox, 1967). No attempt was made to introduce changes in subunit tertiary structure accompanying the quaternary transition (Perutz, 1970).

Intrinsic pK Values. There are three categories of proton binding sites. The first class comprises all groups with normal pK_{int}: terminal carboxyl, 3.60; Asp, 4.00; Glu, 4.50; heme propionic acid, 4.00; His N^{π}, 6.00; His N^{τ}, 6.60; terminal amino, 7.00; Cys, 9.00; Tyr, 10.00; Lys, 10.40; and Arg, 12.00. Choice of the appropriate intrinsic pK value between the two nitrogen atoms in histidine depends on the preponderant exposure of one or the other, as indicated by their solvent accessibilities (Botelho et al., 1978). The only deviation from the referenced data is for the hemoglobin amino terminal group, taken here as 7.00 rather than 8.00 (Botelho et al., 1978; Matthew et al., 1978b). The pK_{int} of 7.00, unusually low for a peptide terminal amine, is apparently attributable to unique nonelectrostatic interaction inherent to the native hemoglobin structure (Gros & Bauer, 1978). The second class of sites refers to other groups with abnormal pK_{int} values as the result of hydrogen bonding or of other chemical involvement. Here, pK_{int} was adjusted by adding 0.50 for Lys and Tyr groups or by subtracting 0.50 for Glu and Asp groups. The charge was assigned to the appropriate atom either on the basis of the hydrogen-bonding pattern or on the degree of solvent accessibility.

The third class is that of masked, that is nontitratable, groups. These cases were identified by specific chemical or structural evidence. Thus, analysis of hydrogen ion titration curves indicates that, of the 10 histidine residues in the α chain and 9 in the β chain of human hemoglobin, a total of 10–12 groups per dimer are titratable (Tanford & Nozaki, 1966; Bucci et al., 1968); similar work on the comparison of various components and species of hemoglobin shows that His-116β is masked (Janssen et al., 1970; Janssen, 1970) while His-117β is titratable (Schneider et al., 1969). Proton NMR measurements show that a total of 11 histidine groups can be identified as titratable in human deoxyhemoglobin and 10 can be identified in oxyhemoglobin (per dimer), and the following groups have been identified by NMR assignment: His-2β, His-143β, and His-146β (Ho & Russu, 1978). In addition, His-58α and His-63β and His-87α and His-92β are masked through their approximation to the heme, being the distal and proximal histidines, respectively. Six groups are nontitratable through masking during association of the dimer subunits: His-103α, His-122α, and His-97β. These sites are involved in hydrogen bonding between subunits (Fermi, 1975; Perutz, 1977). Static accessibility data are in accord with crystal-

Table II: Summary of Evidence for Masking of Tetrameric Hemoglobin Histidine Residues

titratable	masked
His-20α^{e}	His-58$\alpha^{a,e}$
His-45α^{e}	His-87$\alpha^{a,e}$
His-50α^{f}	His-103$\alpha^{d,e}$
His-72α^{e}	His-122$\alpha^{d,e}$
His-89α^{e}	
His-112α^{f}	
His-2$\beta^{b,e}$	His-63$\beta^{a,e}$
His-77β^{e}	His-92$\beta^{a,e}$
His-117$\beta^{c,f}$	His-97β^{d}
His-143$\beta^{b,e}$	His-116$\beta^{c,d,e}$
His-146$\beta^{b,e}$	

[a] Proximal or distal histidine (Fermi, 1975; Perutz, 1970). [b] Proton nuclear magnetic resonance (Ho & Russu, 1978; Fung & Ho, 1975). [c] Potentiometric titration (species comparison) (Janssen, 1970; de Bruin & Janssen, 1973). [d] Crystallographic evidence (Fermi, 1975; Perutz, 1970, 1977). [e] Static solvent accessibility (SA) (Lee & Richards, 1971; Matthew et al., 1978a). [f] Low SA, due to surface electrostatic pairing (Matthew, 1978).

lographic evidence that His-103α, His-122α, and His-116β are buried within the dimer at the $\alpha\beta$ interface and that His-97β is in the $\alpha_1\beta_2$ dimer–dimer interface. His-50α and His-112α also have low solvent accessibilities, but these groups are in electrostatic association with neighboring surface side chains of Glu-30α and Glu-27α, respectively. In summary, only the proximal and distal, and four interface histidines per dimer, have been considered as masked in the present calculations. A summary of the arguments and a list of the groups are given in Table II.

Cys-104α and Cys-112β and Tyr-42α, Tyr-140α, and Tyr-145β are also masked, the former on the basis of lack of reactivity toward sulfhydryl reagents (Rosemeyer & Huehns, 1967) and the latter through involvement in intra- or interchain hydrogen bonding within the molecule (Fermi, 1975). In practice, these groups do not significantly affect titration curves below pH 10.

Solvent Accessibilities. The procedure for calculating accessible surface area of a group X in the protein relative to that in the model tripeptide Ala-X-Ala has already been described (Lee & Richards, 1971; Matthew, 1978; Matthew et al., 1978a). It was applied in the present work to obtain the fractional SA_j values for every proton binding site in human hemoglobin, at the monomer, dimer, and tetramer levels, a total of 182 groups, for the deoxy- as well as oxyhemoglobin. The SA values were kept within the practical limits of 0.02, for a buried group, to 0.98 for an exposed one. The calculated quantities are listed together with other data in Tables III–V. Of the 91 groups in each $\alpha\beta$ dimer, 21 groups show SA changes between monomer, dimer, and tetramer, and 13 groups show SA differences between the deoxy and the oxy tetramer structures.

Summary. The method may now be summarized. It was assumed that the solution structures of deoxyhemoglobin and oxyhemoglobin are the same as their crystal structures and that these structures remain essentially unaltered within the range of conditions investigated. Given the atomic coordinates, electrostatic free energies and solvent accessibilities were calculated for each titratable group, the latter factor being introduced to account for the unique dielectric environment of individual groups at the protein–solvent interface. The hemoglobin molecule was taken as an equivalent sphere, the tetramer having a radius of 27.0 Å. Dielectric constants at 25 °C were taken as $D_i = 4.00$ and $D = 78.5$. All 182 titratable groups were considered, 91 per $\alpha\beta$ dimer.

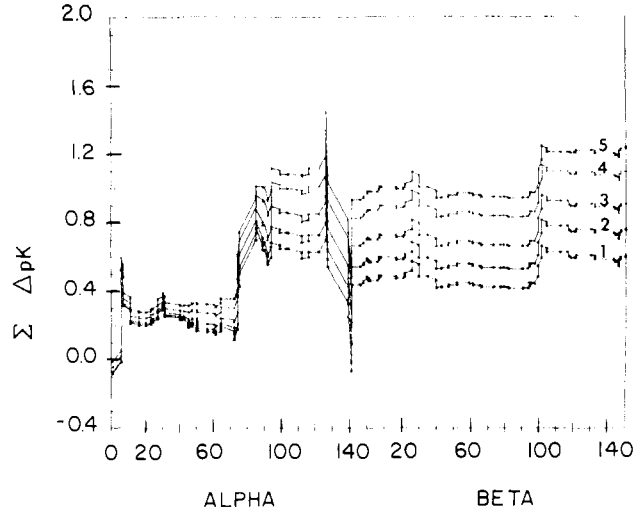

FIGURE 2: Summation plots of intramolecular electrostatic contributions, ΔpK_{ij}, defined in eq 5, to the value of pK_i of the amino acid residue Val-1α in deoxyhemoglobin tetramer, computed at $I = 0.01$ M and at pH 5.0, 6.0, 7.0, 8.0, and 9.0 (curves 1–5, respectively). The sums are cumulative, showing the residue sequence numbers of the groups in their α and β chains. A contribution attributed to a particular site represents the summed effect of that site from each dimer. In the case of Val-1α, being very near the hemoglobin tetramer symmetry axis, the effects are nearly equal between dimers. The net values at the extreme right represent the electrostatic potential acting on the deoxyhemoglobin Val-1α site at the given pH.

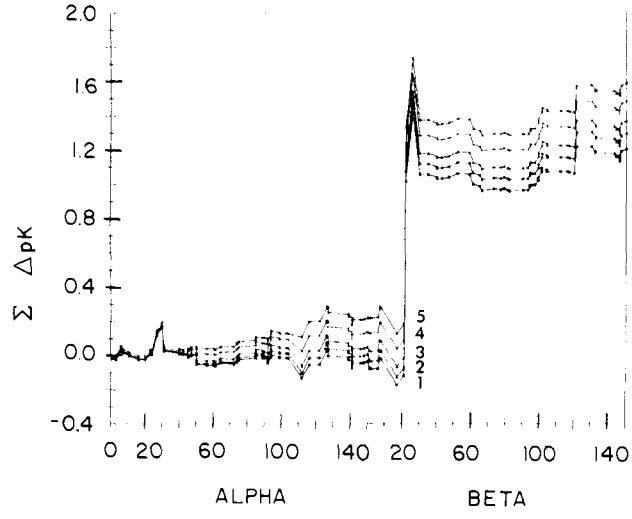

FIGURE 3: Summation plots, corresponding to those in Figure 2 and under the same conditions, showing electrostatic contributions to the value of pK_i of the amino acid residue His-117β. The sharp rises at Glu-22β and Glu-26β illustrate the dominating effect of close interaction with these two negative sites, yielding the extremely high pK_i value of 8.2 for His-117β at pH 9.0. In contrast to Val-1α the His-117β site is off the dyad axis, and the effects are primarily the result of one dimer site, the second being generally at a greater r_{ij}.

Results and Discussion

pH Dependence of j Site Contributions to pK_i. At a given pH, the unique protein charge distribution confers an effective pK_i value on each titratable site i. pK_i is determined by the interplay of the protein's entire charge complement. The Coulombic influence on site i exerted by each one of the other sites j is proportional to the charge Z_j and to the extent of its burial within the protein molecule $(1 - SA_j)$, but it is inversely proportional to intercharge distance r_{ij}.

Figures 2 and 3 show the final iterative calculation of pK_i at five pH values for two sites in deoxyhemoglobin tetramer, Val-1α and His-117β, respectively. The electrostatic con-

Table III: The Thirty-Three Unique Carboxyl Group Sites in Human Tetrameric Hemoglobin

chain	residue	amino acid	atom	static accessibility[a] monomer	dimer	tetramer deoxy	tetramer oxy	pK_{int}	pK_i at pH 6.0 (I = 0.10) deoxy	pK_i at pH 6.0 (I = 0.10) oxy
α	6	Asp	OD2	0.02				4.0	3.19	2.91
α	47	Asp	OD2	0.50				3.5	3.40	3.36
α	64	Asp	OD1	0.46				3.5	3.45	3.48
α	74	Asp	OD1	0.26				4.0	3.02	2.99
α	75	Asp	OD2	0.44				4.0	3.87	3.86
α	85	Asp	OD1	0.10				4.0	2.49	2.53
α	94	Asp	OD1	0.88	0.88	0.05	0.05	4.0	4.9	4.21
α	126	Asp	OD2	0.79	0.24	0.05	0.05	4.0	3.15	2.69
β	21	Asp	OD2	0.74				4.0	3.93	3.92
β	47	Asp	OD1	0.82				4.0	3.98	4.00
β	52	Asp	OD1	0.82				4.0	4.02	4.02
β	73	Asp	OD2	0.90				4.0	3.98	3.95
β	79	Asp	OD1	0.85				4.0	3.69	3.63
β	94	Asp	OD1	0.12				4.0	3.18	2.98
β	99	Asp	OD1	0.76	0.76	0.05	0.05	4.0	4.81	4.29
α	23	Glu	OE1	0.53				4.5	4.17	4.15
α	27	Glu	OE1	0.10				4.5	2.38	2.34
α	30	Glu	OE1	0.27				4.5	2.83	2.79
α	116	Glu	OE2	0.33				4.5	4.25	4.24
β	6	Glu	OE2	0.95				4.5	4.52	4.51
β	7	Glu	OE2	0.05				4.0	3.08	3.08
β	22	Glu	OE1	0.38				4.5	3.24	3.22
β	26	Glu	OE1	0.14				4.0	2.44	2.39
β	43	Glu	OE2	0.95				4.5	4.21	4.34
β	90	Glu	OE1	0.84				4.5	4.6	4.49
β	101	Glu	OE1	0.29	0.29	0.09	0.28	4.0	4.48	3.35
β	121	Glu	OE2	0.42				4.0	2.74	2.73
α	141	Arg	OXT	0.69	0.69	0.41	0.35	3.5	2.96	2.19
β	146	His	OXT	0.76	0.76	0.22	0.50	3.5	3.45	3.55
α		heme	02	0.80				4.0	3.98	3.98
α		heme	02	0.69				4.0	3.45	3.46
β		heme	01	0.50				4.0	3.84	3.81
β		heme	01	0.77				4.0	4.05	4.04

[a] Static accessibility values are listed for the monomer. Differences in static accessibility for dimer and tetramer are included where applicable. The assigned pK_{int} and computed pK_i at pH 6.0 for the deoxy and oxy tetramers are tabulated.

tributions to pK_i are summed according to the formalism of eq 4 as

$$pK_i = (pK_{int})_i - \sum_{j \neq i} \Delta pK_{ij} \quad (5)$$

where

$$\Delta pK_{ij} = Wm_{ij}z_iZ_j/(2.30kT)$$

In Figures 2 and 3 the individual ΔpK_{ij} contributions are summed cumulatively from left to right along the x axis following the j site residue number in its respective chain, so that at the extreme right the level corresponds to the total electrostatic contribution to the effective magnitude of pK_i for site i at the given pH. Every step in each figure represents the summed effects of the given residue in both of the pairs of α or β chains.

The charge Z_i is positive for residues Val-1α and His-117β, the examples shown in the figures. It follows from eq 4 and 5 that a rise in the level reflects the influence of negatively charged sites (Z_j is negative), while a drop in level corresponds to pK_i depression under the influence of positively charged sites. Nearly constant levels in the plots represent sections of the chain sequence whose residues are either nontitratable, neutral at that pH, or such that the combination of the effects of Z_j, SA_j and r_{ij} tends to balance out.

Figure 2 also shows that, at I = 0.01 M and over the range of pH 5–9, the computed electrostatic effect on Val-1α totals from 0.1 to 1.2 which, based on pK_{int} = 7.00, yields an effective pK_i which varies from 7.6 at pH 5 to 8.2 at pH 9. The midtitration value, $pK_{1/2}$, is 8.1. On the whole, it is seen that there are a large number of small contributions from other groups determining the resultant pK_i value for Val-1α.

In contrast, Figure 3 shows that the electrostatic effect on His-117β is dominated by very strong interaction with two negative groups, Glu-22β and Glu-26β. A pK rise of 1.2–1.6 occurs, yielding the extremely high pK_i values of 7.8 at pH 5 and 8.2 at pH 9 (based on pK_{int} = 6.60). Here again, lesser effects from more distant groups are not negligible.

Computed pK_i Values. The effective pK_i values (eq 4) were obtained for each titratable site in human deoxyhemoglobin and oxyhemoglobin tetramers, as a function of pH and ionic strength. The sites are tabulated in three sets, corresponding to the groups that titrate largely below pH 6 (carboxyl, in Table III), the groups that titrate above pH 9 (ε-amino, sulfhydryl, tyrosyl, and guanidyl in Table IV), and finally the groups that titrate mainly within the more neutral range of interest, pH 6–9 (histidine and terminal amino, Table V).

Table III lists the 33 unique carboxyl group sites, according to the α- or β-chain residue position in the sequence and the specific electronegative proton-binding atom in the given residue chosen on the basis of its greater solvent accessibility. The SA fractional values are listed respectively for the deoxyhemoglobin monomers, dimers, and tetramers and for the oxyhemoglobin tetramers. SA for monomers are given for all the entries; they are omitted for the other structures except where differences occur so that the subunit interface residues and those affected by the quaternary transition stand out. The table also lists the pK_{int} value adopted in each case as described above, and the last two columns give the computed effective pK_i values, under the selected conditions of pH 6.0 and ionic strength I = 0.10, for the deoxy and the oxy tetramers.

Table IV: The Thirty-Seven Unique Cysteine, Tyrosine, Lysine, and Arginine Residues

chain	residue	amino acid	atom	static accessibility[a] monomer	dimer	tetramer deoxy	tetramer oxy	pK_{int}	pK_i at pH 9.0 ($I = 0.10$) deoxy	pK_i at pH 9.0 ($I = 0.10$) oxy
α	104	Cys	SG	0.13	0.05	0.05	0.05	M		
β	93	Cys	SG	0.10				9.0	10.54	10.24
β	112	Cys	SG	0.94	0.05	0.05	0.05	M		
α	24	Tyr	OEE	0.25				10.0	10.56	10.55
α	42	Tyr	OEE	0.35	0.35	0.05	0.05	M		
α	140	Tyr	OEE	0.05				M		
β	35	Tyr	OEE	0.68	0.26	0.26	0.26	10.0	11.4	11.00
β	130	Tyr	OEE	0.05				10.0	10.35	10.31
β	145	Tyr	OEE	0.05				10.0	10.95	10.71
α	7	Lys	NZ	0.44				10.4	11.72	11.70
α	11	Lys	NZ	0.51				10.4	10.77	10.75
α	16	Lys	NZ	0.82				10.4	11.22	11.21
α	40	Lys	NZ	0.79	0.79	0.59	0.78	10.4	11.60	10.75
α	56	Lys	NZ	0.89				10.4	10.85	10.84
α	60	Lys	NZ	0.98				10.4	10.75	10.74
α	61	Lys	NZ	0.80				10.4	10.83	10.82
α	90	Lys	NZ	0.98				10.4	10.55	10.60
α	99	Lys	NZ	0.88	0.79	0.79	0.57	10.4	11.42	10.99
α	127	Lys	NZ	0.71	0.71	0.40	0.12	10.4	12.48	13.03
α	139	Lys	NZ	0.18				10.4	12.03	11.95
β	8	Lys	NZ	0.86				10.4	10.59	10.57
β	17	Lys	NZ	0.36				10.4	11.53	11.52
β	59	Lys	NZ	0.90				10.4	10.48	10.48
β	61	Lys	NZ	0.73				10.4	10.65	10.65
β	65	Lys	NZ	0.90				10.4	10.66	10.65
β	66	Lys	NZ	0.65				10.4	11.04	11.02
β	82	Lys	NZ	0.72				10.4	10.46	9.40
β	95	Lys	NZ	0.95				10.4	10.81	10.75
β	120	Lys	NZ	0.95				10.4	10.60	10.58
β	132	Lys	NZ	0.40				10.4	11.74	11.86
β	144	Lys	NZ	0.54				10.4	10.72	10.54
α	31	Arg	NH2	0.54	0.07	0.07	0.07	12.0	13.6	13.55
α	92	Arg	NH2	0.84	0.84	0.44	0.81	12.0	12.30	12.21
α	141	Arg	NH2	0.95	0.95	0.34	0.17	12.0	14.0	13.97
β	30	Arg	NH1	0.27	0.07	0.07	0.07	12.0	13.77	13.72
β	40	Arg	NH2	0.95	0.95	0.39	0.10	12.0	12.60	12.69
β	104	Arg	NH1	0.71	0.71	0.71	0.28	12.0	13.56	12.52

[a] Static accessibilities and pK_{int} follow the format of Table III with the introduction of "M" to designate masked sites.

Table V: The Twenty-One Unique Histidine and Terminal Valine Sites in Human Hemoglobin

chain	residue	amino acid	atom	static accessibility[a] monomer	dimer	tetramer deoxy	tetramer oxy	pK_{int}	$pK_{1/2}$ ($I = 0.1$) deoxy	$pK_{1/2}$ ($I = 0.1$) oxy
α	20	His	NE2	0.98				6.6	6.75	6.74
α	45	His	NE2	0.26				6.6	6.84	6.83
α	50	His	ND1	0.05				6.0	7.47	7.43
α	58	His	ND1	0.05				M		
α	72	His	ND1	0.55				6.0	6.32	6.31
α	87	His	NE2	0.05				M		
α	89	His	NE2	0.56				6.6	7.15	7.19
α	103	His	NE2	0.92	0.05	0.05	0.05	M		
α	112	His	NE2	0.05				6.6	7.71	7.68
α	122	His	NE2	0.69	0.05	0.05	0.05	M		
β	2	His	NE2	0.95				6.6	6.53	6.52
β	63	His	NE2	0.05				M		
β	77	His	NE2	0.95				6.6	6.58	6.53
β	92	His	NE2	0.05				M		
β	97	His	NE2	0.92	0.92	0.65[b]	0.89	M		
β	116	His	NE2	0.95	0.05	0.05	0.10	M		
β	117	His	NE2	0.19				6.6	7.75	7.72
β	143	His	NE2	0.76	0.76	0.76	0.35	6.6	6.07	4.0
β	146	His	NE2	0.27				6.6	8.48	8.21
α	1	Val	N	0.72	0.72	0.44	0.44	7.0	7.56	7.30
β	1	Val	N	0.23				7.0	7.00	6.80

[a] The format follows that established in Tables III and IV with the exception of reporting $pK_{1/2}$ instead of a pK_i. "M" designates masked site. [b] H_2O cross-link not included (Perutz, 1977).

The results in Table III, last two columns, show that hardly any of the carboxylic groups will be significantly protonated at pH 6.0. The nearest exceptions are Asp-94α and Asp-99β; these examples illustrate the magnitude of pK_i shifts at pH

6.0 and $I = 0.10$ that occur in some cases from the change in quaternary structure. Large effects of quaternary structural changes also appear for Asp-126α and Glu-101β. In electrostatic terms, the differences in free energy of dissociation of a group between deoxy and oxy tetramers reflect differences in the summation term in eq 4, effects which will themselves vary with pH and ionic strength.

Table IV lists results for the 37 unique cysteine, tyrosine, lysine, and arginine side chains in the same format as Table III. A few more groups here show significant changes in SA values between the deoxy- and oxyhemoglobin tetramers. In the last two columns, pK_i values are listed at pH 9.0 and ionic strength 0.10 M. Hardly any of this set of groups appears to become significantly deprotonated at pH 9, except Lys-82β for which the computed pK_i is 10.46 in the deoxy tetramer but 9.40 in the oxy tetramer. Other major effects of quaternary change are listed for Lys-40α, Arg-104β, Tyr-35β, Lys-99α, and Lys-127α.

Table V deals with the central set of 19 unique histidine residues and 2 terminal amino (valine) groups. Listing follows the above format except that pK_i is expressed as $pK_{1/2}$, the special value at the pH of half titration for a particular group taken here at ionic strength 0.10 as above. Differences in $pK_{1/2}$ values between the two quaternary forms are seen in His-146β and in the two terminal valines, reflecting free energy changes of about 0.4 kcal/mol. In contrast, His-143β is a striking example of the large effects that accompany stereochemical quaternary change; the drop in $pK_{1/2}$ from 6.07 to less than 4.0 corresponds to 2.9 kcal/mol and reflects the closing in of four positive sites in oxyhemoglobin, the two His-143β and the two Lys-82β side-chain nitrogen atom sites.

The pH region between 6.0 and 9.0 in hemoglobin is clearly dominated by the hydrogen ion equilibria of imidazole and α-amino groups. The computed pK_i values may be tested by comparison with experimental data for these groups. Observed pK values for imidazole ionization in individual histidine residues of hemoglobin have been determined by proton NMR measurements (Ho & Russu, 1978); in some cases the resonances have been assigned by comparison of natural or chemically derived hemoglobin variants. Observed pK values for α-amino group ionization have been determined from ^{13}C NMR measurements for Val-1α and Val-1β (Morrow et al., 1976; Matthew et al., 1977) and from cyanate reaction kinetics (Garner et al., 1975).

Table VI correlates the experimental and theoretical data for the 11 histidine and 2 terminal valine residues involved. The table lists computed $pK_{1/2}$ values at 0.01 and at 0.10 M ionic strength, together with the experimental pK values obtained by proton or ^{13}C NMR measurements under conditions more closely corresponding to 0.10 M. In deoxyhemoglobin 5 out of the 13 and in oxyhemoglobin 4 of the 12 known pK values have been assigned to specific residues. The remaining histidine pK values are aligned in Table VI with the computed $pK_{1/2}$ values, but this tabulation does not imply any attempt at pK assignment. It is apparent that, on the whole, there is reasonable correspondence between the computed and measured pK values, no attempt having been made to improve the fit by adjusting parameters. Discrepancies may be attributed to the uncertainty about experimental ionic strength (the data in the table show that some residues will be more sensitive to ionic strength than others) or to inherent inadequacy of the theoretical model.

Three groups in Table VI merit special attention. Electrostatic calculations for His-143β indicate that $pK_{1/2}$ in oxyhemoglobin is strongly depressed to near 4, which puts it out of the range of experimental measurements and neatly explains the failure to observe a titration for its ^1H NMR resonance in oxyhemoglobin although it displays normal titration in deoxyhemoglobin. The second interesting case is His-146β, for which $pK_{1/2}$ was said to drop markedly (from 8.0 in deoxyhemoglobin to 7.1 in oxyhemoglobin) as a result of tertiary structural rearrangement (Perutz, 1970; Kilmartin et al., 1973; Kilmartin & Rossi-Bernardi, 1973). More recently, a redetermination at lower ionic strength, about 0.1 M, showed only a slight drop from 8.0 to 7.9 (Ho & Russu, 1978), which is much more in line with the theoretical estimate of the effect as listed in Table VI. Finally, Val-1α is known to undergo a drop in $pK_{1/2}$ of nearly 0.7 between deoxy- and oxyhemoglobin, and it is also known to be a binding site for Cl^- ion at the 0.1 M level (Arnone et al., 1967; O'Donnell et al., 1978). If an anion is placed in the tertiary deoxyhemoglobin structure between Val-1α and Arg-141α, electrostatic calculations yield a $pK_{1/2}$ value of 8.02, at $I = 0.10$ M, and $\Delta pK_{1/2}$ for the quaternary transition becomes 0.73 which is in agreement with the experimental value. Further support for this result is provided by the independent study of terminal valine groups by the cyanate kinetic method which yields a $pK_{1/2}$ for Val-1α in deoxyhemoglobin of 7.8 and in carbonmonoxyhemoglobin of 7.0 (Garner et al., 1975).

The pK values for histidine residues in both forms of human hemoglobin fall within a higher range of pH than is the case in the myoglobin where only one histidine residue has its $pK_{1/2}$ over 7 and where as many as three fall below 6 (Botelho et al., 1978). In terms of eq 4, the electrostatic summation term is positive at the pH corresponding to $pK_{1/2}$ for nine sites in deoxy- and for 8 sites in oxyhemoglobin. In sperm whale myoglobin, by contrast, only one of the eight titratable histidines is under a positive net electrostatic effect. The basis of the difference between the two pK patterns resides in the distribution of positively and negatively charged groups and in their varying degrees of accessibility to solvent. The

Table VI: Individual Site $pK_{1/2}$ Values, Theoretical and Experimental[a]

residue and chain	deoxyhemoglobin theoretical I = 0.01	deoxyhemoglobin theoretical I = 0.10	deoxyhemoglobin exptl	oxyhemoglobin theoretical I = 0.01	oxyhemoglobin theoretical I = 0.10	oxyhemoglobin exptl
His-146β	9.00[f]	8.48[f]↝	8.1[b,c]	8.52	8.21↝	7.9[b,c]
His-117β	8.08	7.75	8.2[b]	7.98	7.72	8.0[b]
His-112α	8.14	7.71	7.6[b]	8.04	7.68	7.5[b]
His-50α	7.87	7.47	7.2[b]	7.67	7.43	7.5[b]
His-89α	7.50	7.15	7.18[b]	7.46	7.20	7.2[b]
His-45α	7.11	6.84	7.18[b]	7.00	6.83	7.0[b]
His-20α	6.90	6.75	6.95[b]	6.86	6.74	6.7[b]
His-77β	6.58	6.58	6.75[b]	6.43	6.53	6.6[b]
His-72α	6.52	6.32	6.60[b]	6.46	6.31	6.0[b]
His-2β	6.53	6.53↝	6.38[b,c]	6.43	6.52↝	6.51[b,c]
His-143β	6.03	6.07↝	6.25[b,c]	3.73	4.00	not obsd[b]
Val-1α	8.10	7.56↝	7.83[d]	7.64	7.29↝	7.16[d]
Val-1β	7.13	7.00↝	6.91[d]	6.60	6.80↝	7.00[e]

[a] Deoxy- and oxyhemoglobin theoretical $pK_{1/2}$ values at two ionic strengths are compared with experimentally observed $pK_{1/2}$ values. Theoretical and experimental values are correlated with specifically assigned sites indicated with an arrow. An ionic strength of 0.10 M most closely compares with experimental conditions. [b] Observed by proton NMR (Ho & Russu, 1978). [c] Assigned by variant and chemical modification with proton NMR (Ho & Russu, 1978). [d] Observed and assigned by carbon-13 NMR (Morrow et al., 1976; Matthew et al., 1977). [e] Observed by kinetic methods (Garner et al., 1975). [f] His-146· · ·Asp-94 salt-bridge distance of 2.8 Å may be stretched in solution, yielding a slightly lower $pK_{1/2}$.

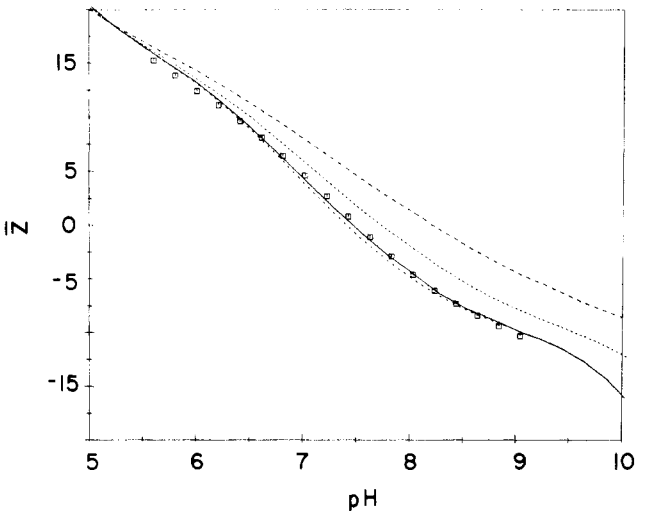

FIGURE 4: The hydrogen ion titration curve of human deoxyhemoglobin showing the variation of net protein charge, $\bar{Z}$, with pH at 25 °C. Experimental data are from Rollema et al. (1975). The computed curves are at three levels of ionic strength: 0.0, 0.01, and 0.10 M (from top to bottom, all broken curves). The full curve is the computed titration curve, protons bound per tetramer, when the effect on hydrogen ion equilibria of Cl^- ion binding at the Val-1α···Arg-141α site is included.

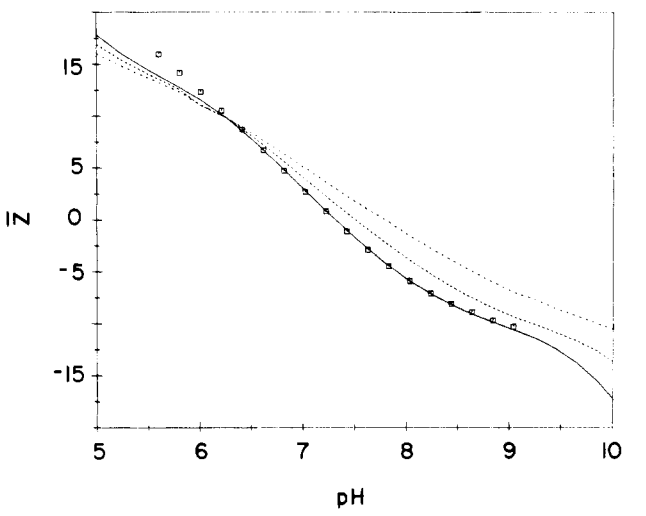

FIGURE 5: The hydrogen ion titration curve of human oxyhemoglobin showing the variation of net protein charge with pH at 25 °C. Experimental data are from Rollema et al. (1975). The computed curves are at three levels of ionic strength, as in Figure 4 except that the solid line is at I = 0.10 M without incorporation of a Cl^- in the computations.

outcome for hemoglobin is to provide buffering capacity with imidazole groups in the physiological pH range of the erythrocyte, while for myoglobin it is to shift that capacity to the appropriate, lower pH range in the muscle cell. These adaptations are comparable in functional importance and in scope within the protein structure to those that determine the oligomeric form of the one protein and the monomeric form of the other.

Titration Curve of Deoxyhemoglobin. The theoretical hydrogen ion titration curve of the hemoglobin tetramer is formed by summing electrostatic contributions from every charged site in the molecule. The groups involved, 91 per dimer, have been listed in Tables III–V.

Figure 4 shows the computed net protein charge, $\bar{Z}$, varying with pH from pH 5 to 10 at 25 °C, at three ionic strength levels, 0.0, 0.01, and 0.1 M (broken curves, top to bottom, respectively). Since, as noted above, specific binding of a Cl^- ion between Val-1α and Arg-141α has already been established, a computed (full) curve that includes Cl^- at 0.1 M ionic strength is also shown in Figure 4 together with experimental data obtained at about 0.1 M chloride concentration (Rollema et al., 1975). Titration data reported for the Bohr effect at I = 0.01 M (de Bruin et al., 1974) substantiate the predicted ionic strength behaviors of deoxyhemoglobin (Figure 4) and oxyhemoglobin (Figure 5). Agreement between theory and experiment is good. Inclusion of Cl^- binding is seen to have a perceptible effect which, if anything, improves the fit. This may be taken as further support for the reality of Cl^- binding to this specific site in deoxyhemoglobin.

The effect of ionic strength on the titration curve brings out an uncommon feature, in that the crossover region is near the acid end at pH 5. Human deoxyhemoglobin A has its isoionic point near pH 7.4, and it is around that region that the net protein charge would normally be expected to be nearly independent of ionic strength (Tanford, 1961). Since the monomeric hemoprotein myoglobin shows classical titration behavior in this respect (Shire et al., 1974a), the question arises as to whether this special feature in hemoglobin may be a consequence of its quaternary structure or of its charge configuration. This question is explored in detail in the following paper in this issue (Matthew et al., 1979).

Titration Curve of Oxyhemoglobin. The theoretical hydrogen ion titration curve of human oxyhemoglobin A, calculated as above, is shown in Figure 5, at 25 °C and at ionic strength levels of 0.0, 0.01, and 0.10 M. At these low salt concentrations there is no direct experimental evidence for a specific anion binding site in oxyhemoglobin; the Cl^- ion of deoxyhemoglobin has therefore been kept out of the calculations here. Figure 5 also includes the experimental titration data in 0.1 M KCl (Rollema et al., 1975). Agreement between theory and experiment is seen to be very good, except in the region of pH below about 6. However, it is known that the dissociation of oxyhemoglobin tetramer into dimer is acid driven (Riggs & Atha, 1976), and it is likewise possible that other conformational or specific salt effects occur at low pH. Discrepancy under these conditions is perhaps not unexpected. Nevertheless, no attempt was made to alter the calculations so as to obtain an apparent improvement in the fit below pH 6.

The effect of ionic strength on the titration curve is shown in Figure 5. The isoionic point for human oxyhemoglobin is near pH 7.2; the computed titration curves intersect near pH 6.2. In comparison with the deoxyhemoglobin case, this result reflects a more nearly normal distribution of charges in the human oxyhemoglobin molecule. Similar behavior has been reported for horse hemoglobin (Orttung, 1970); in a theoretical study of the titration curve of horse oxyhemoglobin, isoionic point near pH 7.1, the crossover region occurred near pH 6.5. The corresponding computation for horse deoxyhemoglobin was not given.

Derivative Titration Curves. Plotting the first derivative of a titration curve provides direct information about inflections and about other features which may not be readily discernible in the ordinary plot. The derivative or differential plot can be particularly useful when the titratable groups of the protein fall neatly into distinct acidic, neutral, and basic regions, as is the case in hemoglobin. It is common practice to plot the form $-\Delta pH/\Delta\bar{Z}$ vs. $\bar{Z}$, so that the maximum buffering capacity appears as a minimum.

The theoretical curves in this form for deoxyhemoglobin and for oxyhemoglobin are shown in Figures 6 and 7, respectively, in each case at two ionic strengths, 0.01 and 0.10 M. Since

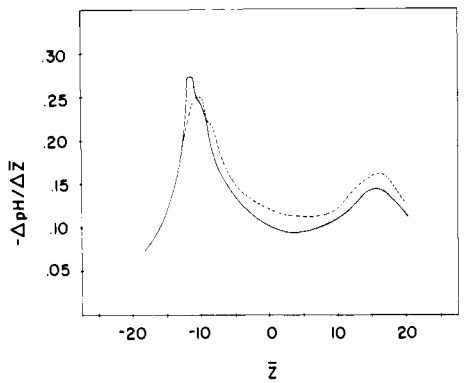

FIGURE 6: Differential (first derivative) theoretical titration curve of human deoxyhemoglobin tetramer taken from the computer data of Figure 4, at ionic strengths 0.01 and 0.10 M (upper and lower curves, respectively). At I = 0.10 M, which corresponds more closely to experimental conditions, the two maxima are separated by 13 charges representing the titration of 11 histidine and 2 valine residues (per dimer) within the pH range of 6–9.

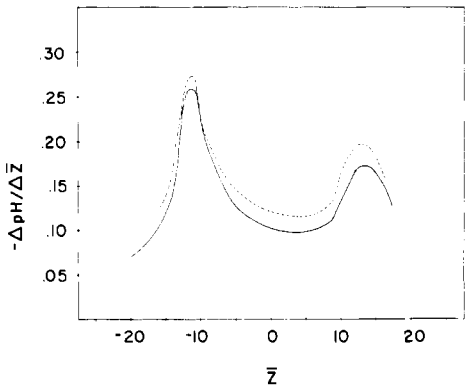

FIGURE 7: Differential (first derivative) theoretical titration curve of human oxyhemoglobin tetramer taken from the computed data of Figure 5 and plotted as Figure 6. The two maxima are separated by 12 charges representing the titration of 10 histidine and 2 valine residues. His-143β, with its pK of 4.0, does not titrate in this region.

agreement between theory and experiment has already been established, the experimental data have been omitted from Figures 6 and 7 for clarity.

The main features of these derivative curves are the two maxima and the broad central trough, the latter indicating that the region of strong protein buffering occurs as expected near the isoionic point. The maxima confirm what the foregoing calculations showed, namely, that the groups of the central pH region titrate separately from the groups at either extreme. The separation of the two maxima gives the number of titratable sites in this pH range; at 25 °C and 0.10 M ionic strength, it is 25.6 charges in deoxyhemoglobin and 23.5 charges in oxyhemoglobin tetramers, corresponding to 13 groups and 12 groups, respectively, per dimer. Table VI lists 11 histidine and 2 valine groups per dimer that titrate within this range in deoxyhemoglobin. In oxyhemoglobin, the special group His-143β becomes strongly acidic, its p$K_{1/2}$ dropping to 4.0, and its titration within the central range is not observed, in agreement with the derivative curve. The results are therefore readily explained, and the use of derivative curves in discerning finer points in the data is demonstrated.

Conclusion. The present electrostatic treatment of hemoglobin is successful. By use of the static accessibility modification of the Tanford–Kirkwood model, a simple and efficient computational procedure yields quantitative and qualitative results in agreement with experimental data. This is particularly satisfying since non-Coulombic effects and arbitrary curve fitting were excluded. The introduction of a solvent accessibility parameter apparently corrects the model adequately so that the smooth protein–solvent boundary of the model is able to mimic the real protein surface. The assumption that the solution structure of hemoglobin throughout the pH range of interest is essentially that of the crystal seems to hold reasonably well. Minor perturbations may of course occur in solution and could be expected to alter charge configurations. Specific chloride ion binding is an example that has been taken into account above.

The working electrostatic model for the hemoglobin tetramer molecule adapts easily to a variety of problems and enables one to evaluate electrostatic contributions to such diverse phenomena as the Bohr effect, the binding of CO_2, 2,3-diphosphoglycerate ions, or other effectors, amino acid substitutions in hemoglobins of various animal species or mutant human hemoglobins, and any known tertiary or quaternary structural change. Some aspects of these effects will be dealt with in the following paper in this issue (Matthew et al., 1979).

Acknowledgments

The advice of Professors D. A. McQuarrie and F. M. Richards is gratefully acknowledged. Professor C. Ho and I. M. Russu are thanked for making their data available prior to publication. The assistance of Dr. R. J. Wittebort and S. H. Friend at various stages of the development was greatly appreciated. Without the excellent computing facility at Indiana University, none of this work would have been possible.

References

Arnone, A., O'Donnell, S., & Schuster, T. (1976) *Fed. Proc., Fed. Am. Soc. Exp. Biol. 35*, 1604.

Beetlestone, J. G., & Irvine, D. H. (1964) *Proc. R. Soc. London, Ser. A 277*, 414.

Botelho, L. H., Friend, S. H., Matthew, J. B., Lehman, L. D., Hanania, G. I. H., & Gurd, F. R. N. (1978) *Biochemistry 17*, 5197.

Bucci, E., Fronticelli, C., & Ragatz, B. (1968) *J. Biol. Chem. 243*, 241.

Cox, J. (1967) *J. Mol. Biol. 28*, 151.

de Bruin, S. H., & Janssen, L. H. M. (1973) *Biochim. Biophys. Acta 295*, 490.

de Bruin, S. H., Rollema, H. S., Janssen, L. H. M., & van Os, G. A. J. (1974) *Biochem. Biophys. Res. Commun. 58*, 210.

Fermi, G. (1975) *J. Mol. Biol. 97*, 237.

Fung, L. W. M., & Ho, C. (1975) *Biochemistry 14*, 2526.

Garner, M. H., Bogardt, R. A., Jr., & Gurd, F. R. N. (1975) *J. Biol. Chem. 250*, 4398.

Gros, G., & Bauer, C. (1978) *Biochem. Biophys. Res. Commun. 80*, 56.

Hill, T. L. (1956) *J. Phys. Chem. 60*, 253.

Ho, C., & Russu, I. M. (1978) in *Clinical and Biochemical Aspects of Hemoglobin Abnormalities* (Caughey, W. S., Ed.) pp 179–193, Academic Press, New York.

Janssen, L. H. M. (1970) Ph.D. Thesis, Universiteit Te Nijmegen.

Janssen, L. H. M., de Bruin, S. H., & van Os, G. H. J. (1970) *Biochim. Biophys. Acta 221*, 214.

Kilmartin, J. V., & Rossi-Bernardi, L. (1973) *Physiol. Rev. 53*, 836.

Kilmartin, J. V., Breen, J. J., Roberts, G. C. K., & Ho, C. (1973) *Proc. Natl. Acad. Sci U.S.A. 70*, 1246.

Lee, B., & Richards, F. M. (1971) *J. Mol. Biol. 55*, 379.

Linderstrøm-Lang, K. (1924) *C. R. Trav. Lab. Carlsberg 15*, 70.

Matthew, J. B. (1978) Ph.D. Thesis, Indiana University, Bloomington, IN.
Matthew, J. B., Morrow, J. S., Wittebort, R. J., & Gurd, F. R. N. (1977) *J. Biol. Chem. 252*, 2234.
Matthew, J. B., Hanania, G. I. H., & Gurd, F. R. N. (1978a) *Biochem. Biophys. Res. Commun. 81*, 410.
Matthew, J. B., Friend, S. H., Botelho, L. H., Lehman, L. D., Hanania, G. I. H., & Gurd, F. R. N. (1978b) *Biochem. Biophys. Res. Commun. 81*, 416.
Matthew, J. B., Hanania, G. I. H., & Gurd, F. R. N. (1979) *Biochemistry* (following paper in this issue).
Morrow, J. S., Matthew, J. B., Wittebort, R. J., & Gurd, F. R. N. (1976) *J. Biol. Chem. 251*, 477.
Muirhead, H., Cox, J. M., Mazzarella, L., & Perutz, M. F. (1967) *J. Mol. Biol. 28*, 117.
O'Donnell, S., Mandaro, R., & Schuster, T. (1978) *Biophys. J. 21*, 201a.
Orttung, W. H. (1968) *J. Phys. Chem. 72*, 4066.
Orttung, W. H. (1969) *J. Am. Chem. Soc. 91*, 162.
Orttung, W. H. (1970) *Biochemistry 9*, 2394.
Perutz, M. F. (1970) *Nature (London) 228*, 726.
Perutz, M. F. (1977) *BioSystems 8*, 261.
Riggs, A., & Atha, D. H. (1976) *J. Biol. Chem. 251*, 5537.
Rollema, H. S., de Bruin, S. H., Janssen, L. H. M., & van Os, G. A. J. (1975) *J. Biol. Chem. 250*, 1333.
Rosemeyer, M. A., & Huehns, E. R. (1967) *J. Mol. Biol. 25*, 253.
Schneider, R. G., Alperin, J. B., Brimhall, B., & Jones, R. T. (1969) *J. Lab. Clin. Med. 73*, 616.
Shire, S. J., Hanania, G. I. H., & Gurd, F. R. N. (1974a) *Biochemistry 13*, 2967.
Shire, S. J., Hanania, G. I. H., & Gurd, F. R. N. (1974b) *Biochemistry 13*, 2974.
Shire, S. J., Hanania, G. I. H., & Gurd, F. R. N. (1975) *Biochemistry 14*, 1352.
Tanford, C. (1957) *J. Am. Chem. Soc. 79*, 5340.
Tanford, C. (1961) *Physical Chemistry* of *Macromolecules*, Chapter 8, Wiley, New York.
Tanford, C., & Kirkwood, J. G. (1957) *J. Am. Chem. Soc. 79*, 5333.
Tanford, C., & Nozaki, Y. (1966) *J. Biol. Chem. 241*, 2832.
Tanford, C., & Roxby, R. (1972) *Biochemistry 11*, 2192.
Wittebort, R. J., Rothgeb, T. M., Szabo, A., & Gurd, F. R. N. (1979) *Proc. Natl. Acad. Sci. U.S.A. 76*, 1059.

Electrostatic Effects in Hemoglobin: Bohr Effect and Ionic Strength Dependence of Individual Groups†

James B. Matthew,‡ George I. H. Hanania,§ and Frank R. N. Gurd*

ABSTRACT: The electrostatic treatment applied in the preceding paper in this issue [Matthew, J. B., Hanania, G. I. H., & Gurd, F. R. N. (1979) *Biochemistry* (preceding paper in this issue)] to the titration behavior of individual groups in human deoxyhemoglobin and oxyhemoglobin was applied to the computation of the alkaline Bohr effect at various values of ionic strength. The enhanced proton binding of deoxyhemoglobin in the pH range of 6–9 was accounted for at ionic strength 0.01 M by the effects of the unique charge distributions of ionizable groups in the two quaternary states. At ionic strength 0.10 M the effects of 2–4 bound anions had to be considered in addition in the deoxyhemoglobin charge configuration. At the higher ionic strength 10 groups per tetramer contributed to the Bohr effect, whereas 28 groups were contributory at the lower ionic strength. The ionic strength dependence of individual groups in the two tetrameric structures as well as in the α-chain monomer was explained in terms of the electrostatic treatment. This examination showed that the differences in electrostatic behavior of deoxy- and oxyhemoglobin follow from particular dissymmetries in their configurations with respect to charge and static solvent accessibility.

The preceding paper in this issue (Matthew et al., 1979) introduced the application to human hemoglobin of a modified discrete-charge electrostatic model. The characteristics of the protein–solvent interface are taken into account by an approximation incorporating the static solvent accessibility of each charged site as computed from the crystallographic structure of the protein. A basic feature of the model is that the charge and the pK_i of each ionizable group vary with pH and ionic strength. Hence, the charge-related properties of the protein incorporate, to some degree, individual contributions from all these groups. Examples of the computed contribution of each ionizable group in the hemoglobin molecule to the pK_i of a given group were presented for several different pH values. The computed pK_i values under certain conditions of interest were tabulated for all ionizable groups in the deoxy- and oxyhemoglobin tetramers, and correspondence with observed values was established in those cases where comparison was possible. The titration curves computed as functions of ionic strength for the deoxyhemoglobin and oxyhemoglobin tetrameric structures agreed with experimental values.

The present paper explores in greater detail the application of the model to elucidating differences in the electrostatic behavior of the deoxyhemoglobin and oxyhemoglobin structures. To account for the alkaline Bohr effect, that describes the excess of proton binding by deoxyhemoglobin relative to oxyhemoglobin in the physiological pH range (Bohr et al., 1904), it is necessary to invoke the intervention of at most two bound chloride ions (per $\alpha\beta$ dimer) in addition to the direct

† From the Department of Chemistry, Indiana University, Bloomington, Indiana, 47405. *Received November 9, 1978; revised manuscript received February 16, 1979.* This is the 105th paper in a series dealing with coordination complexes and catalytic properties of proteins and related substances. For the preceding paper see Matthew et al. (1979). This work was supported U.S. Public Public Health Service Research Grant HL-05556. J.B.M. was supported by U.S. Public Health Service Grant T01 GM-1046.

‡ Present address: Department of Molecular Biophysics and Biochemistry, Yale University, New Haven, CT.
§ Present address: Department of Chemistry, American University of Beirut, Beirut, Lebanon.

0006-2960/79/0418-1928$01.00/0